A BASELINE STUDY OF THE EFFECT OF FRESHWATER BIOFILMS IN HYDRAULIC CONDUITS

ANDREW F. BARTON[1], JANE E. SARGISON[1], GREGORY J. WALKER[1], JON E. OSBORN[2] and PAUL A. BRANDNER[3]

[1]School of Engineering, University of Tasmania Private Bag 65, Hobart, Tasmania, 7001, Australia.
[2]School of Geography and Environmental Studies Private Bag 76, Hobart, Tasmania, 7001, Australia.
[3]Faculty of Maritime Transport and Engineering, Australian Maritime College Launceston, Tasmania, 7248, Australia.
(Tel: +61-3-6226-2142, Fax: +61-3-6226-7247, e-mail: afbarton@utas.edu.au)

Abstract

A program is underway at the University of Tasmania investigating ways to control biological growths in hydraulic conduits. The broad aim of this research is to minimise the effects of biological growths to optimize conduit performance and maintenance procedures, and increase the economic return from existing hydraulic infrastructure. This paper presents results from experiments carried out on a newly constructed re-circulating water tunnel purpose built to investigate the effect of freshwater biofilms in hydraulic conduits. A baseline study of boundary layer velocity profiles and total drag measurements of a specially prepared rough test plate has been conducted to determine the plate's roughness characteristics. Experimental measurements from the water tunnel are complemented with three-dimensional physical roughness data obtained from innovative photogrammetric methods. The roughness data from the water tunnel and photogrammetry are compared and are shown to agree by within 20%.

Keywords: Biofouling; Biofilms; Boundary layer; Roughness; Friction; Headloss; Hydraulic conduit; Hydro-electric scheme

1. INTRODUCTION

The carrying capacity of hydraulic conduits is known to deteriorate over time due to the growth of biological material on internal surfaces. The friction and roughness effects of these growths on the flow are not well understood. Schultz (1999) found the equivalent sandgrain roughness height of biofilms to exceed the physical height. This problem of biological fouling (biofouling) can afflict most types of hydraulic conduits, be they for water supply (Brown 1903-1904; Minkus 1954), drainage (Bland *et al.* 1975; Perkins and Gardiner 1985) or hydro-electric power generation (Barton *et al.* 2004; Brett 1980; Picologlou *et al.* 1980; Pollard and House 1959).

A multi-faceted program is underway at the University of Tasmania investigating ways to control biofouling in hydraulic conduits and to conduct fundamental research on the roughness and friction characteristics of freshwater biofilms. Biofilms differ from standard engineering materials as they have complex topographies and visco-elastic properties. A multidisciplinary approach has been applied to the research program with aspects including paint trials to see which have an ability to prevent or minimise biological growth (not unlike anti-fouling paints used in the shipping industry, though more environmentally appropriate) using a variety of paint types in different flow conditions in both pipes and canals; field studies investigating the headloss of biofouled and cleaned conduits and determining the respective friction factors and equivalent sandgrain roughness for comparison; microbiological studies investigating biofilm communities, diversity and possible methods to control their development; an experimental laboratory program using a newly built water tunnel to investigate the friction and roughness characteristics of biofilms in a controlled way; and an innovative photogrammetry program using close range techniques to map the three-dimensional physical surface of biofilms.

This paper a presents a baseline study of total drag measurements and boundary layer velocity profiles of a specially prepared test plate to determine the plate roughness characteristics. Experimental measurements from the water tunnel are compared to three-dimensional physical roughness data obtained from close range photogrammetric methods. The broad aim of this research is to determine, in the first instance, how well the measured three-dimensional roughness data (with fundamental data reduction) compares to the roughness effects measured in the water tunnel. Later in the research program test plates with biofilms at various states of maturity and hydraulic conditioning (i.e. grown in the field in predominantly high or low velocity regions) will be studied in this manner.

Results presented in this paper show that the methods used to determine the equivalent sandgrain roughness of the test plate with non-uniform sandgrain type roughness agree to within 20% with the photogrammetric data. These information and measurement techniques will enable optimization of conduit performance and maintenance, minimise the effects of biological growth and increase the economic return from existing hydraulic infrastructure.

2. WATER TUNNEL AND TEST PLATE SURFACE DETAILS

The water tunnel used to conduct the measurements for the present study is a newly constructed special purpose design. The detailed design and calibration of the water tunnel is the subject of a future paper. The water tunnel is a re-circulating design consisting of de-swirl sections upstream and downstream of the pump, cascading bends, a two stage diffusion, a honey comb and wire mesh flow conditioner and a two-dimensional contraction all to ensure a controlled and uniform flow within the working section. The water tunnel design was based on the principles of aeronautical wind tunnels whereby techniques can be used to determine shear forces and boundary layer information (see Bradshaw and Pankhurst 1964). Figure 1 shows dimensions of the working section and a general arrangement of the two-dimensional

contraction attached upstream of the working section. For the present study this is where all measurements were taken. Table 1 provides a summary of the water tunnel characteristics.

Table 1. Water tunnel characteristics

Maximum flow rate	0.24 m^3/s
Maximum working section velocity	Up to 2 m/s
Dimensions of working section	0.2m high by 0.6m wide by 2.2m long
Typical plate Reynolds number range	1×10^6 to 3×10^6 for 1-2m/s and 10-30°C
Working section material	All 30mm thick acrylic

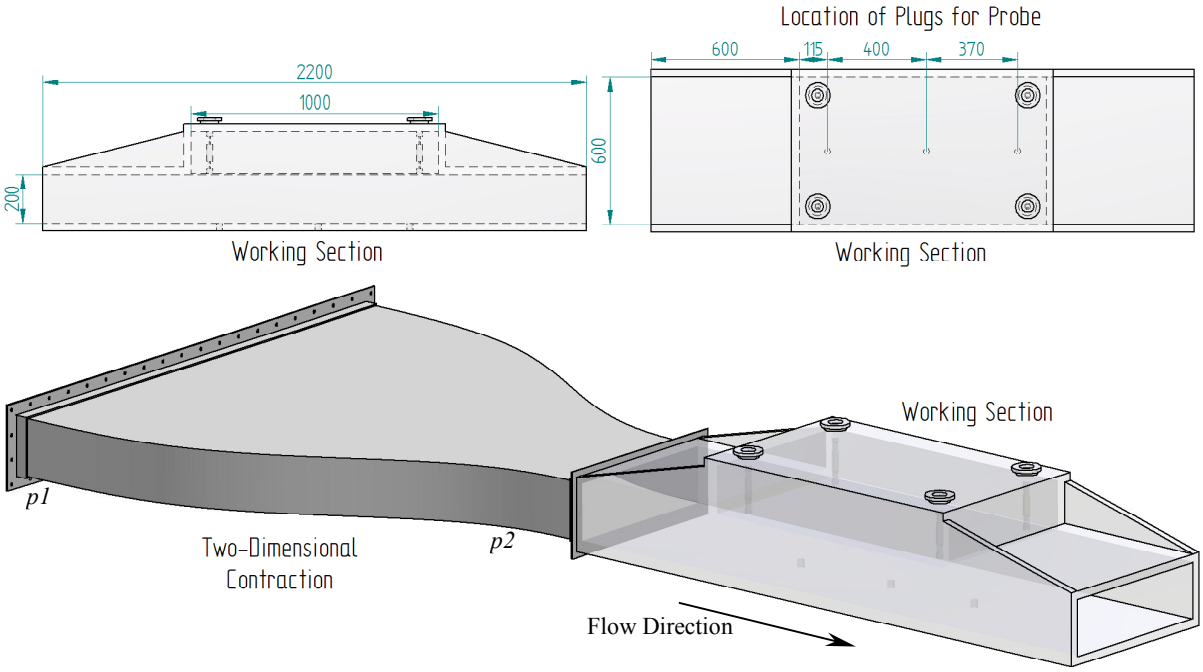

Fig. 1 Working section details showing upstream two-dimensional contraction

The working section flow characteristics is designed to duplicate the wall friction range in full-scale field situations ranging from low velocity open channels to high pressure and velocity penstock pipelines. Using this information a test plate size of 997mm long and 597mm wide is used. The plate is made of 3mm thick stainless steel. The rough finish on the plate shown in Fig. 5b was artificially prepared using a base of special tar with allowed the bonding of horticultural propagating sand (ranging in diameter by approximately 0.5-3mm) uniformly across the surface. This finish provided good optical texture and colour, which was important for the photogrammetry, and provided similar likeness to the fine aggregate in aged concrete, typical of open channels in Tasmanian hydropower generation infrastructure.

3. INSTRUMENTATION

A force balance arrangement was used for the total drag measurements. The test plate is suspended from the lid of the working section by four precision machined stainless steel flexures. A MTI Weigh Systems single ended shear beam load cell (model MTI-4856-SB) is attached to the lid of the working section and linked by a load transfer rod to the acrylic backing of the test plate. The flexures ensure a one-dimensional transfer of force through the load transfer rod to the load cell, which is connected to a Mann Industries strain gauge transmitter and then computer for data acquisition using LabView software. This arrangement was calibrated in place in the water tunnel with low friction pulleys and known weights.

All pressure measurements were taken using a Validyne Engineering variable reluctance differential pressure transducer (model DP15). Static wall pressures were measured at upstream and downstream tappings on the contraction, p_1 and p_2 respectively (see Fig. 1), and at the location of a Pitot probe at either plug 1, 2 or 3, p_{Plug} (see Fig. 2). Total pressure for the boundary layer traverse was measured using a Pitot probe, p_{Pitot}, at either plug 1, 2 or 3. The Pitot probe outside diameter was 1mm, with a 6mm stainless steel support held in place by a plug with a gland seal. Each pressure was measured in turn using a solenoid switching arrangement connected to one side of the differential pressure transducer. The contraction pressure, p_1, was used as the reference pressure.

Three holes (plug 1, 2 or 3) are located in the bottom of the working section to accommodate probes for measurement shown in Fig. 2. The center of the holes are located at distances of 115mm, 515mm and 885mm downstream of the leading edge of the test plate as shown in Fig. 1. The tip of the Pitot probe is 20mm upstream of the main stem of the probe support making the probe traverses 95mm, 495mm and 865mm downstream of the leading edge of the test plate. The probe was attached to a digital precision height gauge for accurate placement.

4. RESULTS FOR THE ROUGH TEST PLATE

There are many difficulties in directly measuring the shear stress with rough plates. This involves the need to determine the wall shear velocity, u^*, indirectly as the use of a Preston tube, for example (see Patel 1965), is not feasible on a rough surface. Another issue is the wall origin, y_0. A wall origin error, ε, often has to be introduced to create a virtual origin, $y_0 + \varepsilon$, to accurately determine wall shear velocity. These issues are discussed by Perry *et al.* (1969) and Schultz (1998). Temperature effects are also a concern, as changes in Reynolds number for a small volume water tunnel with large pump, such as that used for this paper, are significant. It is preferable to monitor temperature and alter pump speed accordingly to conduct measurements at constant Reynolds number to avoid these problems.

4.1 TOTAL DRAG

Total drag measurements were conducted at intervals in pump speed and corresponding working section mean velocities. The measured contraction pressure differential was

calibrated to give the mean working section velocity. The total drag force on the test plate was measured as a voltage and acquired by computer using the LabView software. The voltage was then converted to a force (N) from previous calibrations.

In order to determine the total friction drag coefficient, C_D, on the test plate, it is necessary to know the state of the boundary layer at the start of the test panel. For a smooth test plate (following the smooth wall working section upstream of the test plate) the drag coefficient can be determined using Eq. 1, where it is assumed that the virtual origin of the turbulent boundary layer starts at the inlet to the working section (end of the contraction). For the roughened test plate, the drag coefficient is different to the upstream section, and the boundary layer growth is discontinuous at the start of the test panel. For this arrangement an equivalent upstream length, l_{Equiv}, (shown as the dashed line in Fig. 2) is calculated based on the boundary layer thickness measured at plugs 1 and 2 and the upstream distance at the rough plate wall shear stress required to produce the measured boundary layer thickness at the plugs. Once this is determined, Eq. 1 can again be used to determine the average drag due to friction over the plate. This reduction of the data is necessary to account for the fact that the boundary layer already has some initial growth before the start of the test panel as outlined in Fig. 2. This correction is reflected in the adjusted coefficients of drag presented in the results for the total drag measurements in Fig. 3.

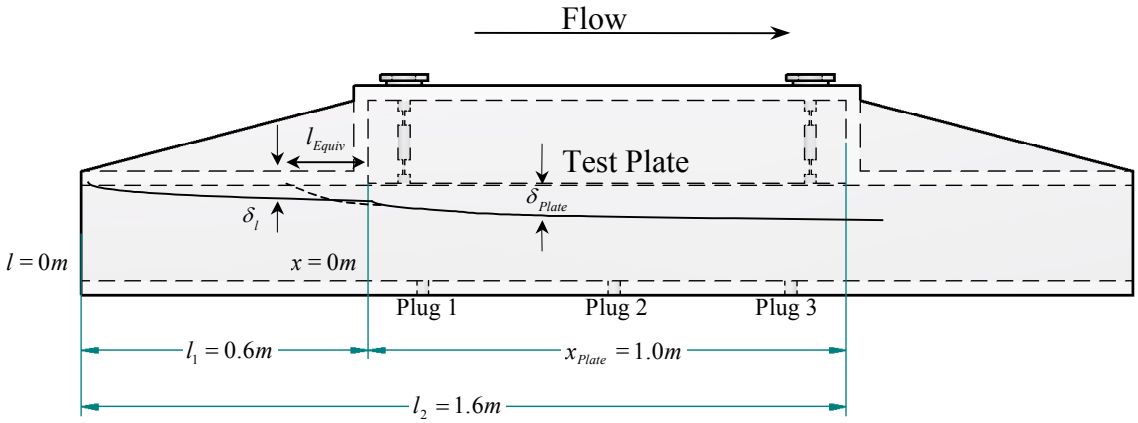

Fig. 2 Assumed turbulent boundary layer development for the calculation of total drag

For a turbulent boundary layer the total drag force equals:

$$Drag_{(Plate)} = C_{D2}\rho b l_2 \frac{U^2}{2} - C_{D1}\rho b l_1 \frac{U^2}{2} \qquad \text{Eq. 1}$$

where for a rough plate $C_D = \left(1.89 + 1.62\log\frac{l}{k_s}\right)^{-2.5}$ (see Schlichting 1979).

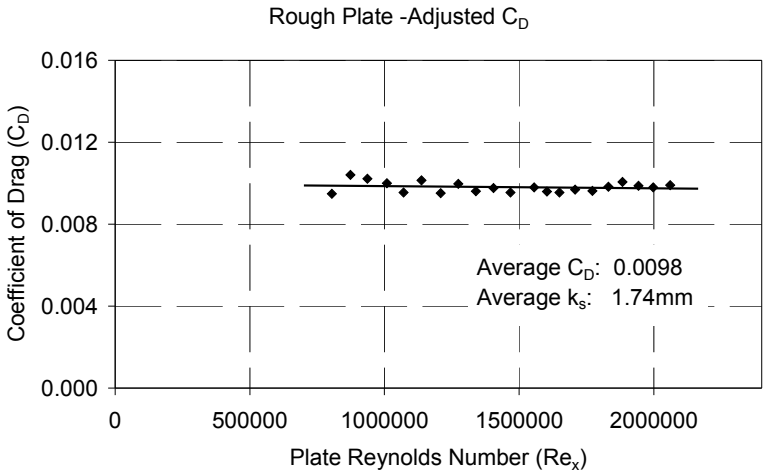

Fig. 3 Results for the total drag on the rough test plate

4.2 BOUNDARY LAYER TIME-MEAN VELOCITY PROFILES

The velocity profiles were measured at plug locations 1-3 along the test plate, and 105 mm upstream of the test panel on the smooth working section wall. The upstream boundary layer had a momentum thickness of 1.74mm indicating that the boundary layer development started near the start of the working section. The profile (shown in Fig. 4) indicates a fully developed turbulent boundary layer at this location.

Results for the velocity profiles over the roughened test panel are presented in Fig. 4. Note the velocity profiles displaying a log-law relationship near the boundary.

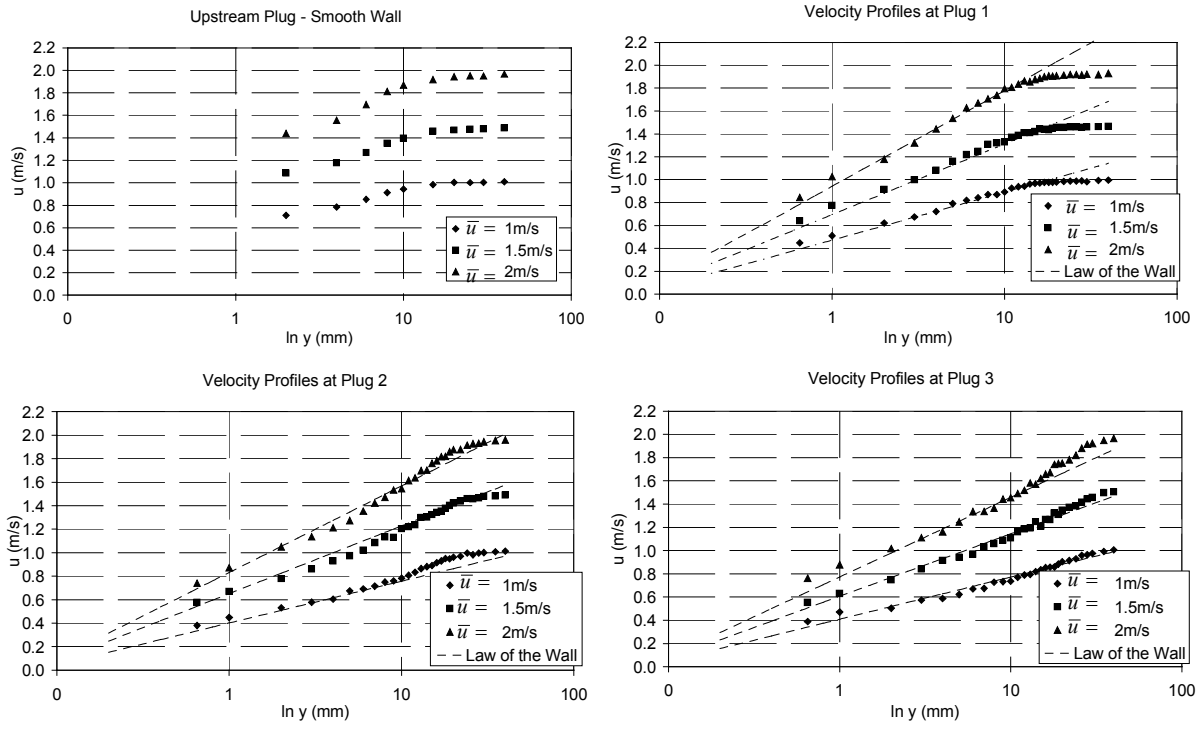

Fig. 4 Time-mean velocity profiles

Using Eq. 2, analysis was undertaken to determine the wall shear velocity, u^*, so the equivalent sandgrain roughness k_s, could be determined. Table 2 shows the results for determination of k_s for three mean flow velocities at plugs 1, 2 and 3.

$$\frac{u}{u^*} = \frac{1}{\kappa}\ln\frac{y}{k_s} + B \qquad \text{Eq. 2}$$

where $\kappa = 0.40$, and $B = 8.5$.

Table 2. Estimated k_s (mm) for each of the measured velocity profiles

	$\bar{u} = 1m/s$	$\bar{u} = 1.5m/s$	$\bar{u} = 2m/s$
Plug 1	2.12	2.03	2.30
Plug 2	2.04	2.85	2.35
Plug 3	2.48	2.40	2.23

5. ROUGHNESS CHARACTERISATION WITH CLOSE RANGE PHOTOGRAMMETRY

A photogrammetric method has been developed that provides localised measurement of surface roughness on test plates, that does not interfere with or damage the surface. This is particularly important for biofilms. The system is suitable for mapping surface roughness over an area of approximately 120mm by 80mm, with a sampling density (X and Y distances) of up to 0.2mm by 0.2mm. Estimated precision in both X and Y is 60 microns, and in Z (height) of 100 microns.

In order to measure biofilm accumulation, it is first necessary to map the surface topography of the clean test plate. Subsequent measurements of the biofilm are then compared with the clean plate. This demands a very high degree of repeatability. The camera rig has been fully calibrated and validated and has developed from the work by Osborn *et al.* (2005).

A sample area of surface roughness of the kind on the test plate used for water tunnel measurements is shown in Fig. 5a. Although not in the exact location, this is the same surface shown in Fig. 5b.

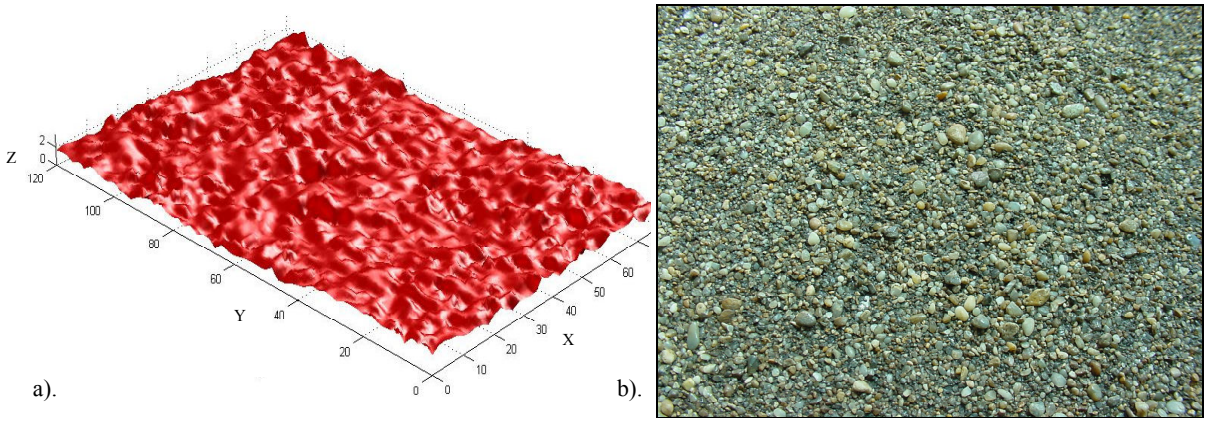

Fig. 5 Digital image of sample area (a), and the artificial surface on the test plate (b)

Five profiles have been selected from the sample area shown in Fig. 5a for further analysis. These are taken at Y = 20, 40, 60, 80 and 100mm, with examples shown in Fig. 6a, b, and c respectively at Y = 20, 60 and 100mm. These Figures are presented plotted about their mean. Fig. 6d is the surface profile at Y = 100mm showing the data positively transformed. Table 3 shows the results for each of the sample profiles and also the total sample area where applicable.

Table 3. Roughness parameters for rough plate

	Roughness Parameters (mm)					Statistical moments			
	Ra	Rq	Rp	Rv	Rt	1st	2nd	3rd	4th
Total Sample Area	0.40	0.50	1.64	-1.61	3.25	(mean)	(variance)	(skewness)	(kurtosis)
Y=20mm	0.34	0.40	0.99	-0.78	1.77	0.78	0.16	0.16	-0.48
Y=40mm	0.25	0.34	1.11	-0.57	1.69	0.57	0.12	0.93	1.60
Y=60mm	0.35	0.43	1.11	-0.57	1.96	0.85	0.19	0.06	-0.21
Y=80mm	0.45	0.55	1.06	-1.38	2.44	1.38	0.30	-0.24	-0.21
Y=100mm	0.31	0.39	0.66	-0.93	1.59	0.93	0.15	-0.26	-0.29

Analysis was undertaken according to Whitehouse (2002) and Table 4 defines the terms used.

Table 4. Definition of roughness parameters

Roughness parameters	Statistical moments
Rq = root mean square (RMS)	**1st** (mean) = arithmetic mean or average
Ra = mean of magnitude of deviation of profile from mean line	**2nd** (variance) = a measure of dispersion among the sample population
Rv = maximum depth of profile below mean line of sample length	**3rd** (skewness) = a measure of symmetry of the profile about the mean line
Rp = maximum height of profile above mean line of sample length	**4th** (kurtosis) = a measure of sharpness or flatness of profile
Rt = maximum peak to valley height of profile of sample length	

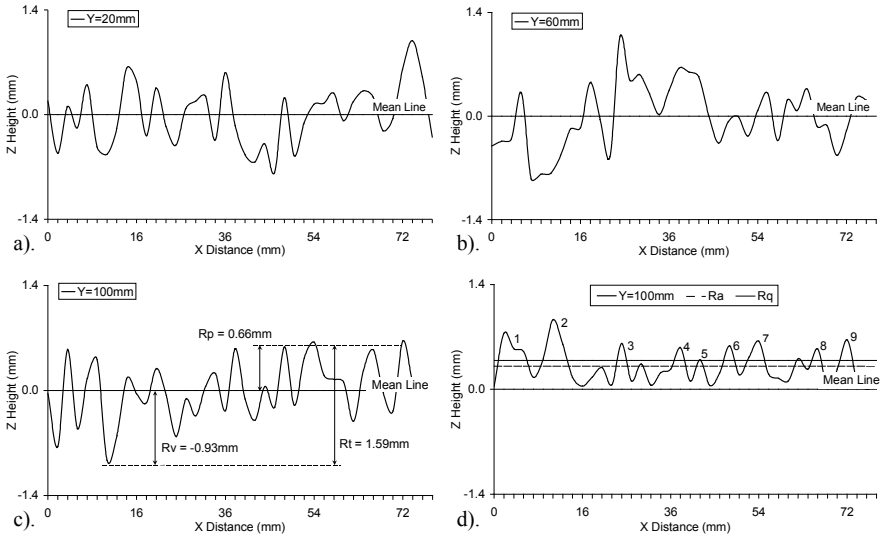

Fig. 6 Sample profiles for Y = 20, 60 and 100mm, with further analysis shown for profile at Y = 100mm

A specialist operator is required to obtain the roughness data from any sample test surface. The turn around time for each sample is relatively quick, with the sample required only for a short time to take the stereo-photographs. This is useful for measurement of biofilms, which need to be kept wet out of water and to have minimum handling to remain viable.

6. FURTHER TUNNEL CAPABILITIES AND RESEARCH DIRECTION

Results described in this paper are for a clean rough test plate. A study program is already underway which involves the investigation of the effect of biofilms and biofouling in general on the efficiency of hydraulic conduits. Current studies are directed towards freshwater biofilms and their roughness and friction characteristics at various stages of growth by using test plates with biofilms grown in the field.

Also being investigated is the hydraulic performance of paints as an option to refurbish conduits, and looking at their potential to minimise biological growths. In addition to time-mean velocity profiles with Pitot probes and total drag measurements with the force balance rig, multi hole and hot film probes will be used for three-dimensional velocity and turbulence measurement.

This paper has provided a general overview of the biofouling research program underway at the University of Tasmania, and given results for a baseline study involving a newly built water tunnel. The water tunnel design and calibration and also further details of the data reduction method will be the subject of future more specialised papers.

7. SUMMARY OF RESULTS

A summary of the average equivalent sandgrain roughness k_s is provided in Table 5. This shows a comparison of the various methods used to obtain the roughness information.

Table 5. Average k_s values

	Total Drag	Velocity Profiles	Photogrammetry (from Rt)
Average k_s (mm)	1.74	2.31	1.89

8. DISCUSSIONS

A new capability now exists to measure roughness, friction and boundary layer characteristics of surfaces with complex roughness. This will be particularly useful for the characterisation of the friction effects due to biofilms in freshwater hydraulic conduits.

Results show that the equivalent sandgrain roughness determined by the total friction drag and time-mean velocity boundary layer measurements is comparable to the photogrammetric roughness data, with results agreeing within 20% (see Table 5). This is encouraging, as although not a completely uniform roughness as used by Nikuradse (1933), the artificially rough plate is still a sandgrain type surface. In reality, the expected sandgrain roughness values are dependent on shape factors as well as the distribution of roughness elements. This

is reflected in the variable uniformity of the roughness elements shown in the photogrammetry data where Rt (also the grain diameter) ranged from 1.59mm for a sample profile, to 3.25mm for the total sample area. The results validate the measurement techniques described generally this paper.

An overview of a larger research program on biofouling involving field studies, paint trials, microbiological studies together with the experimental water tunnel measurements and close range photogrammetric surface mapping of roughness has also been introduced. Each aspect of the research program compliments another, and will be important to develop the necessary holistic approach to create solutions to the biofouling problem.

9. CONCLUSIONS

A new water tunnel, analogous to boundary layer wind tunnel facilities, has been successfully used to measure the total drag and time-mean velocity boundary layer for a rough plate. Innovative photogrammetric methods have been used to measure the three-dimensional physical roughness of the test plate surface. This has proven to be an effective technique for studying the roughness and compares well to the experimental water tunnel measurements.

The path is now set for further studies on the effect of biofilms in hydraulic conduits. The combination of water tunnel measurements and the photogrammetry physical roughness data provides a flexible approach to determining the skin friction characteristics of test plates on which biofilms will grow.

ACKNOWLEDGEMENTS

The writers would like to thank Hydro Tasmania for industry support, in particular Tony Denne. The work completed by Mark Morfew in obtaining the roughness data from the samples provided is also gratefully acknowledged.

REFERENCES

Barton, A. F., Sylvester, M. W., Sargison, J. E., Walker, G. J. and Denne, A. B. (2004). "Deterioration of Conduit Efficiency Due to Biofouling". *8th National Conference on Hydraulics in Water Engineering*, 13-16 July, ANA Hotel Gold Coast, Queensland, Australia.

Bland, C. E. G., Bayley, R. W. and Thomas, E. V. (1975). "Some Observations on the Accumulation of Slime in Drainage Pipes and the Effects of These Accumulations on the Resistance to Flow." *Public Health Engineering*: 21-28.

Bradshaw, P. and Pankhurst, R. C. (1964). "The Design of Low-Speed Wind Tunnels." *Prog. Aero. Sci.* 5: 1.

Brett, T. M. (1980). "Head-Loss Measurements on Hydroelectric Conduits." *ASCE Journal of the Hydraulics Division* HY1: 173- 190.

Brown, J. C. (1903-1904). "Deposits in Pipes and Other Channels Conveying Potable Water." *The Insitution of Civil Engineers - Minutes of Proceedings* CLVI(Part II): 1-17.

Minkus, A. J. (1954). "Deterioration of the Hydraulic Capacity of Pipelines." *New England Water Works Association* LXVIII(1): 1-10.

Nikuradse, J. (1933). Laws of Flow in Rough Pipes. Washington, National Advisory Committee for Aeronautics. Technical Memorandum 1292.

Osborne, J. E., Bae, Y.-S., Grenness, M., Sargison, J. E., Barton, A. F., Sprent, A. S., Walker, G. J. and Bendall, T. (2005). "Mapping Surface Biofilms to Improve the Efficiency of Water Conveyance". *Spatial Sciences Congress*, Melbourne, Spatial Sciences Institute of Australia.

Patel, V. C. (1965). "Calibration of the Preston Tube and Limitations on Its Use in Pressure Gradients." *Journal of Fluid Mechanics* 23(Part 1): 185-208.

Perkins, J. A. and Gardiner, I. M. (1985). "The Hydraulic Roughness of Slimed Sewers." *Intstitution of Civil Engineers* 79: 87-104.

Perry, A. E., Schofield, W. H. and Joubert, P. N. (1969). "Rough Wall Turbulent Boundary Layers." *Journal of Fluid Mechanics* 37(Part 2): 383-413.

Picologlou, B. F., Zelver, N. and Charaklis, W. G. (1980). "Biofilm Growth and Hydraulic Performance." *Journal of the Hydraulics Division* HY5: 733-747.

Pollard, A. L. and House, H. E. (1959). "An Unusual Deposit in a Hydraulic Tunnel." *Journal of the Power Division, ACSE* December: 163-171.

Schlichting, H. (1979). Boundary Layer Theory, McGraw-Hill.

Schultz, M. P. (1998). The Effect of Biofilms on Turbulent Boundary Layer Structure, Phd Thesis. Department of Ocean Engineering. Melbourne, Florida Institute of Technology.

Schultz, M. P., Swain, G.W. (1999). "The Effect of Biofilms on Turbulent Boundary Layers." *Journal of Fluids Engineering* 121: 44-51.

Whitehouse, D. (2002). Surfaces and Their Measurement. London, Hermes Penton Science.